

Shape of the $f_0(980)$ in $\gamma\gamma \rightarrow \pi^+ \pi^-$

N. N. Achasov* and G. N. Shestakov†

Laboratory of Theoretical Physics, S. L. Sobolev Institute for Mathematics, 630090, Novosibirsk, Russia
(Received 6 June 2005; published 22 July 2005)

The Belle Collaboration results on the observation of the $f_0(980)$ resonance in the reaction $\gamma\gamma \rightarrow \pi^+ \pi^-$ are analyzed. It is argued that they point to the presence of mechanisms which give rise to a strong distortion of the $f_0(980)$ resonance shape in comparison with the shape of a solitary Breit-Wigner resonance. It is shown that the main factors responsible for the formation of the specific, steplike, shape of the $f_0(980)$ resonance in the $\gamma\gamma \rightarrow \pi^+ \pi^-$ reaction cross section are the $K^+ K^-$ loop mechanism of the $f_0(980)$ coupling to the $\gamma\gamma$ system and the destructive interference between the background and $f_0(980)$ resonance contributions in the $\pi^+ \pi^-$ invariant mass region below the $K^+ K^-$ threshold.

DOI: [10.1103/PhysRevD.72.013006](https://doi.org/10.1103/PhysRevD.72.013006)

PACS numbers: 13.40.-f, 13.60.Le, 13.75.Lb

I. INTRODUCTION

Recently, the Belle Collaboration succeeded in observing a clear manifestation of the $f_0(980)$ resonance in the reaction $\gamma\gamma \rightarrow \pi^+ \pi^-$ [1]. This has been made possible owing to the huge statistics and good energy resolution. Evidence for the $f_0(980)$ production in $\gamma\gamma$ collisions obtained previously by the Mark II [2], CELLO [3], ALEPH [4], Crystal Ball [5,6], and JADE [7] Collaborations was essentially less conclusive [1,8]. The Belle data [1] corresponding to the $f_0(980)$ resonance region are shown in Fig. 1. Figure 1(a) shows the distribution of $e^+ e^- \rightarrow e^+ e^- \pi^+ \pi^-$ and $e^+ e^- \rightarrow e^+ e^- \mu^+ \mu^-$ events, ΔN , in the invariant mass of the $\pi^+ \pi^-$ and $\mu^+ \mu^-$ systems, m , scanned with a 5-MeV-wide step. A distinct peak due to the $f_0(980)$ resonance production in the $\gamma\gamma \rightarrow \pi^+ \pi^-$ channel can be seen in this plot. The peak position $m_{f_0} = 981.2 \pm 0.5$ MeV and its total width $\Gamma = 21.7 \pm 2.1$ MeV were determined in Ref. [1] by fitting the m dependence of ΔN in the $f_0(980)$ region to the incoherent sum of the resonance and background contributions:

$$\Delta N = \frac{4.8\pi A\Gamma}{(m_{f_0}^2 - m^2)^2 + m_{f_0}^2 \Gamma^2} + \Delta N_{BG}, \quad (1)$$

where $\Delta N_{BG} = C_0 + C_1 m + C_2 m^2$ represents a smooth background and the parameter A is the production of the two-photon width $\Gamma_{f_0 \rightarrow \gamma\gamma}$, branching ratio $B(f_0 \rightarrow \pi^+ \pi^-)$, and known factors connected with the detection efficiency and the setup luminosity [1]. The Belle Collaboration plans to report the information on $\Gamma_{f_0 \rightarrow \gamma\gamma}$ after the investigation of the systematic error sources [1]. The Belle data for the $\gamma\gamma \rightarrow \pi^+ \pi^-$ reaction cross section, $\sigma(\gamma\gamma \rightarrow \pi^+ \pi^-)$, in the region $|\cos\theta^*| < 0.6$, where θ^* is the center-of-mass scattering angle of pion, with indication only statistical errors are shown in Fig. 1(b). The comparison of these data with those of the previous Mark II [2] and CELLO [3] experiments is presented in Fig. 1(c).

*Electronic address: achasov@math.nsc.ru†Electronic address: shestako@math.nsc.ru

It should be noted that, according to the Belle data, the $f_0(980)$ resonance manifests itself in the $\gamma\gamma \rightarrow \pi^+ \pi^-$ reaction cross section rather as a jump, or a step, with a width of about 15 MeV and a height of about 11 nb, than as a clear peak; see Fig. 1(b). In connection with this “observation,” as well as bearing in mind some theoretical reasons (see below), we would like to draw attention, especially of the experimentalists, to the fact that Eq. (1) cannot be used to determine the physical characteristics of the $f_0(980)$ resonance from the data on the reaction $\gamma\gamma \rightarrow \pi^+ \pi^-$. First, due to the proximity of the $f_0(980)$ resonance to the $K\bar{K}$ thresholds and its strong coupling to the $K\bar{K}$ channels, the propagator of the form $1/(m_{f_0}^2 - m^2 - im_{f_0}\Gamma)$, with the total width independent of m , cannot be applied in principle to the description of the $f_0(980)$ resonance shape. Second, owing to the $K^+ K^-$ loop mechanism, the two-photon width of the $f_0(980)$ resonance is a sharply varying function of m just in the $f_0(980)$ peak region. Therefore, it cannot be approximated by a constant. And third, one cannot but take into account that the $f_0(980)$ resonance strongly interferes with the considerable S wave background contributions in the $\gamma\gamma \rightarrow \pi^+ \pi^-$ reaction cross section.

In the present paper we analyze in detail the role of basic dynamical mechanisms of the reaction $\gamma\gamma \rightarrow \pi^+ \pi^-$ in the 1 GeV region and elucidate a possible form of the $f_0(980)$ resonance manifestation in this channel. In so doing, we tried to use sufficiently simple, but adequate to the highly not simple physical situation, formulas free of unknown parameters.

The paper is organized as follows. In Sec. II, the $K^+ K^-$ loop mechanism of the $f_0(980) \rightarrow \gamma\gamma$ decay is discussed. This mechanism not only ensures the appreciable distortion of the $f_0(980)$ resonance shape in the reaction $\gamma\gamma \rightarrow \pi^+ \pi^-$ but also automatically yields a reasonable estimate for the absolute magnitude of the $f_0(980)$ production cross section in this channel with the values of the $f_0(980)$ resonance parameters compatible with the data on the other reactions. Thus, we get good reasons to consider the $K^+ K^-$ loop mechanism as a major one of the $f_0(980)$ production

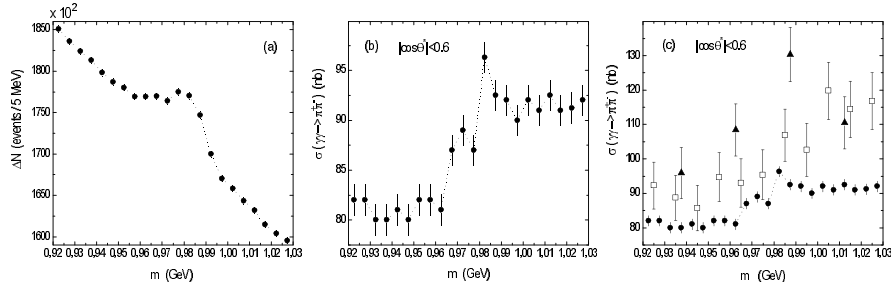


FIG. 1. (a) The Belle data [1] for the invariant mass distribution of $e^+e^- \rightarrow e^+e^-\pi^+\pi^-$ and $e^+e^- \rightarrow e^+e^-\mu^+\mu^-$ events. (b) The Belle data [1] for $\sigma(\gamma\gamma \rightarrow \pi^+\pi^-)$; the quoted errors are statistical only. (c) The comparison of the Belle data [1] for $\sigma(\gamma\gamma \rightarrow \pi^+\pi^-)$ with the analogous data of the Mark II [2] (open squares) and CELLO [3] (full triangles) experiments. The Belle points (full circles) are joined by dotted lines for clearness.

in $\gamma\gamma$ collisions. In Sec. III, a simplest dynamical model for the S wave amplitude of the reaction $\gamma\gamma \rightarrow \pi^+\pi^-$ in the 1 GeV region is examined and the character of the interference between the background and $f_0(980)$ resonance contributions, and thereby a possible resulting shape of the $f_0(980)$ in the $\gamma\gamma \rightarrow \pi^+\pi^-$ channel, is clarified. Most of all the shape obtained resembles a step. This conclusion is supported by the Belle data. A possible manifestation of the $f_0(980)$ resonance in the $\gamma\gamma \rightarrow \pi^0\pi^0$ channel is briefly discussed. The general remarks and conclusions based on the results of our analysis are formulated in Sec. IV.

II. K^+K^- LOOP MECHANISM OF THE $f_0(980) \rightarrow \gamma\gamma$ DECAY

Perhaps, none of the known hadronic resonances can “boast” of such a variety of the forms of its own manifestation that the $f_0(980)$ resonance possesses. The $f_0(980)$ shape in the two-pion decay channel depends in a crucial way on the reaction and varies from dips to peaks. In many respects this is due to the fact that background contributions, usually accompanying the $f_0(980)$ resonance, strongly change in passing from reaction to reaction, which leads in its turn to the change of the interference patterns in the resonance region. But, the even more impressive thing is that there exist reactions in which the $f_0(980)$ production amplitude itself sharply changes just in the $f_0(980)$ peak region. First of all such a phenomenon takes place in the radiative decays $\phi \rightarrow f_0(980)\gamma \rightarrow \pi\pi\gamma$ [9–11]. As predicted theoretically in Ref. [9] and confirmed in the experiments performed at Novosibirsk [12,13] and Frascati [14], these decays are determined by the K^+K^- loop mechanism of the $f_0(980)$ production, $\phi \rightarrow K^+K^-\gamma \rightarrow f_0(980)\gamma \rightarrow \pi\pi\gamma$, the amplitude of which is large, owing to the strong coupling of the $f_0(980)$ to $K\bar{K}$, and changes very rapidly as a function of the two-pion invariant mass near the K^+K^- threshold. The related decay $\phi \rightarrow a_0^0(980)\gamma \rightarrow \eta\pi^0\gamma$ is also determined by the K^+K^- loop mechanism [9,10,13,15–17]. It should be also recalled that the impor-

tant role of this mechanism in the process $\gamma\gamma \rightarrow a_0^0(980) \rightarrow \eta\pi^0$ was shown long ago in Ref. [18]. The above mentioned manifestations of the K^+K^- loop mechanism present important physical evidences in favor of the four-quark ($q^2\bar{q}^2$) nature of the $f_0(980)$ and $a_0^0(980)$ resonances [9,18–20].

The presentation of high quality data from the Belle Collaboration on the reaction $\gamma\gamma \rightarrow \pi^+\pi^-$ provides good reason to discuss in detail the role of the K^+K^- loop mechanism of the $f_0(980)$ resonance production in $\gamma\gamma$ collisions. As we shall show, it is very important, if not determining at all. Note that the process $\gamma\gamma \rightarrow K\bar{K} \rightarrow f_0(980) \rightarrow \pi\pi$ seems to be first mentioned in Ref. [21].

Thus, let us consider the shape of the $f_0(980)$ resonance produced in the reaction $\gamma\gamma \rightarrow \pi^+\pi^-$ via the K^+K^- loop mechanism. This mechanism corresponds to the following sequence of transitions. At first, there takes place the formation of the K^+K^- pair in $\gamma\gamma$ collisions, with the amplitude which near the K^+K^- threshold can be taken in the Born approximation. Then, the K^+K^- system turns into the $f_0(980)$ resonance decaying further into $\pi^+\pi^-$. According this prescription, the corresponding resonant contribution to the $\gamma\gamma \rightarrow \pi^+\pi^-$ reaction cross section can be written as

$$\begin{aligned} \sigma_{f_0}(\gamma\gamma \rightarrow \pi^+\pi^-) &= \frac{8\pi}{m^2} \frac{m\Gamma_{f_0 \rightarrow K^+K^- \rightarrow \gamma\gamma}^{\text{Born}}(m)m\Gamma_{f_0 \rightarrow \pi^+\pi^-}(m)}{|D_{f_0}(m)|^2}. \end{aligned} \quad (2)$$

Here

$$\begin{aligned} \Gamma_{f_0 \rightarrow K^+K^- \rightarrow \gamma\gamma}^{\text{Born}}(m) &= \frac{1}{16\pi m} |M_{f_0 \rightarrow K^+K^- \rightarrow \gamma\gamma}^{\text{Born}}(m)|^2 \\ &= \frac{\alpha^2}{4\pi^2} |I_{K^+K^-}(m)|^2 \frac{g_{f_0 K^+K^-}^2}{16\pi m} \end{aligned} \quad (3)$$

is the width of the $f_0(980) \rightarrow \gamma\gamma$ decay due to the Born K^+K^- loop mechanism, where $\alpha = e^2/4\pi \approx 1/137$ and the function $I_{K^+K^-}(m)$ is [18]

$$I_{K^+K^-}(m) = \begin{cases} \frac{m_{K^+}^2}{m^2} [\pi + i \ln \frac{1 + \rho_{K^+}(m)}{1 - \rho_{K^+}(m)}]^2 - 1, & m \geq 2m_{K^+}, \\ \frac{m_{K^+}^2}{m^2} [\pi - 2 \arctan |\rho_{K^+}(m)|]^2 - 1, & 0 \leq m \leq 2m_{K^+}. \end{cases} \quad (4)$$

The propagator of the $f_0(980)$ resonance with a mass m_{f_0} appearing in Eq. (2) has the form [22]

$$\frac{1}{D_{f_0}(m)} = \frac{1}{m_{f_0}^2 - m^2 + \sum_{a\bar{a}} [\text{Re}\Pi_{f_0}^{a\bar{a}}(m_{f_0}) - \Pi_{f_0}^{a\bar{a}}(m)]}, \quad (5)$$

where $\Pi_{f_0}^{a\bar{a}}(m)$ is the polarization operator of the $f_0(980)$ resonance corresponding to the contribution of the $a\bar{a}$ intermediate state ($a\bar{a} = \pi^+ \pi^-, \pi^0 \pi^0, K^+ K^-, K^0 \bar{K}^0$). For $m \geq 2m_a$,

$$\Pi_{f_0}^{a\bar{a}}(m) = \xi_{a\bar{a}} \frac{g_{f_0 a\bar{a}}^2}{16\pi} \rho_a(m) \left[i - \frac{1}{\pi} \ln \frac{1 + \rho_a(m)}{1 - \rho_a(m)} \right], \quad (6)$$

$\rho_a(m) = (1 - 4m_a^2/m^2)^{1/2}$ [if $0 \leq m \leq 2m_a$, then $\rho_a(m) \rightarrow i|\rho_a(m)|$], $\Gamma_{f_0 \rightarrow a\bar{a}}(m) = \text{Im}\Pi_{f_0}^{a\bar{a}}(m)/m = \xi_{a\bar{a}} g_{f_0 a\bar{a}}^2 \rho_a(m)/16\pi m$ is the width of the $f_0(980) \rightarrow a\bar{a}$ decay, here $\xi_{a\bar{a}} = 1$, if $a \neq \bar{a}$, and $\xi_{a\bar{a}} = 1/2$, if $a = \bar{a}$, and $g_{f_0 \pi^+ \pi^-}^2 = g_{f_0 \pi^0 \pi^0}^2 = 2g_{f_0 \pi\pi}^2/3$, $g_{f_0 K^+ K^-}^2 = g_{f_0 K^0 \bar{K}^0}^2 = g_{f_0 K\bar{K}}^2/2$, where $g_{f_0 \pi\pi}$ and $g_{f_0 K\bar{K}}$ are the coupling constants of the $f_0(980)$ to the $\pi\pi$ and $K\bar{K}$ channels, respectively. Since we are interested in the m region near the $K\bar{K}$ thresholds, we take into account the K^+ and K^0 meson mass difference.

As for the $f_0(980)$ resonance parameters, the available data, together with various model parametrizations, allow wide intervals for their possible values; for example, $m_{f_0} \approx (0.965\text{--}0.99)$ GeV, $g_{f_0 \pi\pi}^2/16\pi \approx (0.065\text{--}0.3)$ GeV², and $g_{f_0 K\bar{K}}^2/16\pi \approx (0.3\text{--}1.6)$ GeV², with the preferred coupling-constant-squared ratio $R = g_{f_0 K\bar{K}}^2/g_{f_0 \pi\pi}^2 \approx 4\text{--}6$, are quite compatible with the data on most reactions of the $f_0(980)$ production [9,10,12–14,22–28]. For further estimates and illustrations of the role of the K^+K^- loop

mechanism, we use, in fact, all the range of possible values of the $f_0(980)$ parameters.

Let us now discuss the two most important features of the K^+K^- loop mechanism which immediately follow from the above formulas. First, as seen from Fig. 2(a), the factor $m\Gamma_{f_0 \rightarrow K^+K^- \rightarrow \gamma\gamma}^{\text{Born}}(m)$ in Eq. (2) sharply decreases just below the K^+K^- threshold, i.e., directly in the $f_0(980)$ resonance region. For instance, it falls relative to the maximum at $m = 2m_{K^+} \approx 0.9873$ GeV by a factor of 1.69, 2.23, 2.75, 3.27, and 6.33 at $m = 0.98, 0.97, 0.96, 0.95$, and 0.9 GeV, respectively. Such a behavior of $m\Gamma_{f_0 \rightarrow K^+K^- \rightarrow \gamma\gamma}^{\text{Born}}(m)$ strongly suppresses the left wing of the $f_0(980)$ resonance peak defined by $1/|D_{f_0}(m)|^2$ in Eq. (2). Second, from Eqs. (2) and (3) it follows that for the K^+K^- loop mechanism the magnitude of $\sigma_{f_0}(\gamma\gamma \rightarrow \pi^+ \pi^-)$ near the maximum, located between m_{f_0} and $2m_{K^+}$, is controlled mainly by the parameter $R = g_{f_0 K\bar{K}}^2/g_{f_0 \pi\pi}^2$ and the value of the function $|I_{K^+K^-}(m)|^2$. For example, if $m_{f_0} < 2m_{K^+}$, then, at $m = m_{f_0}$, $\sigma_{f_0}(\gamma\gamma \rightarrow \pi^+ \pi^-) = \alpha^2 R |I_{K^+K^-}(m)|^2 / [\pi m^2 \rho_\pi(m)]$. Furthermore, at fixed m_{f_0} and R , the $f_0(980)$ resonance shape in $\sigma_{f_0}(\gamma\gamma \rightarrow \pi^+ \pi^-)$ is very insensitive to the absolute values of the coupling constants $g_{f_0 \pi\pi}^2/16\pi$ and $g_{f_0 K\bar{K}}^2/16\pi$. As an illustration we represent in Figs. 2(b) and 2(c) the cross section $\sigma_{f_0}(\gamma\gamma \rightarrow \pi^+ \pi^-)$ for four different sets of the $f_0(980)$ resonance parameters: $m_{f_0} = 0.98$ GeV, $R = 4$, $g_{f_0 K\bar{K}}^2/16\pi = 0.4$ GeV², and 1.2 GeV² (sets A and B), and $m_{f_0} = 0.97$ GeV, $R = 5.33$, $g_{f_0 K\bar{K}}^2/16\pi = 0.533$ GeV², and 1.6 GeV² (sets C and D). For sets A and D the cross section smoothed with a Gaussian mass distribution with the dispersion of 5 MeV (which we have chosen to be equal to the m step in the Belle experiment) is shown in these

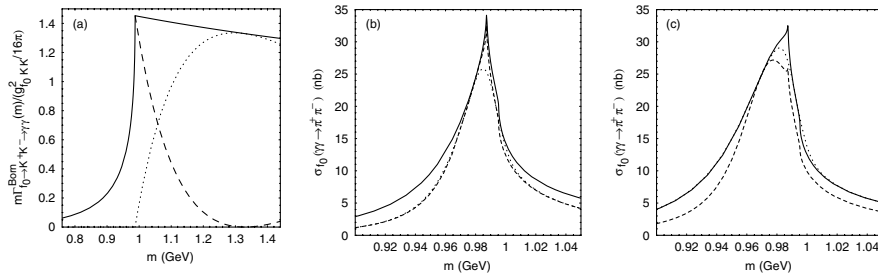


FIG. 2. (a) The solid curve shows $m\Gamma_{f_0 \rightarrow K^+K^- \rightarrow \gamma\gamma}^{\text{Born}}(m)/(g_{f_0 K\bar{K}}^2/16\pi)$ as a function of m , see Eqs. (3) and (4); the dashed and dotted curves above the K^+K^- threshold correspond to the contributions of the real and imaginary parts of the $M_{f_0 \rightarrow K^+K^- \rightarrow \gamma\gamma}^{\text{Born}}(m)$ amplitude to $m\Gamma_{f_0 \rightarrow K^+K^- \rightarrow \gamma\gamma}^{\text{Born}}(m)$, respectively. The dashed, solid curves in (b) and (c) show the cross section $\sigma_{f_0}(\gamma\gamma \rightarrow \pi^+ \pi^-)$ corresponding to the $f_0(980)$ production via the K^+K^- loop mechanism, see Eq. (2), for the $f_0(980)$ parameter sets A, B and C, D, respectively. For completeness, the dotted curves in (b) and (c) show the examples of the cross sections smoothed with a Gaussian mass distribution with the dispersion of 5 MeV for sets A and D, respectively.

figures for completeness. Multiplying the resulting cross section values by a factor 0.6 [in accordance with the fact that the data for $\sigma(\gamma\gamma \rightarrow \pi^+\pi^-)$ correspond to the region $|\cos\theta^*| < 0.6$], we obtain that, owing to the K^+K^- loop mechanism, the $f_0(980)$ resonance can manifest itself in the measured $\gamma\gamma \rightarrow \pi^+\pi^-$ reaction cross section at the level of about 15.5–17.5 nb at the maximum. As is clear from Fig. 1(b), this estimate for the scale of the enhancement due to the $f_0(980)$ resonance contribution to the $\pi^+\pi^-$ production cross section is in reasonable (if not excellent) agreement with the Belle data. Thus, we conclude that the K^+K^- loop mechanism, which actually results from the unitarity condition, can be primarily responsible for the $f_0(980)$ resonance coupling to photons.

It is clear that in there is no sense in speaking about a two-photon width at the resonance point if the two-photon decay width of the resonance varies rapidly within its hadronic width; see Fig. 2(a). For the K^+K^- loop mechanism, it is of interest to evaluate the $f_0(980) \rightarrow \gamma\gamma$ width averaged by the resonance mass distribution in the $\pi\pi$ channel, $\langle \Gamma_{f_0 \rightarrow K^+K^- \rightarrow \gamma\gamma}^{\text{Born}} \rangle_{\pi\pi}$ [18]. By definition,

$$\begin{aligned} \langle \Gamma_{f_0 \rightarrow K^+K^- \rightarrow \gamma\gamma}^{\text{Born}} \rangle_{\pi\pi} &= \int_{m_1}^{m_2} \Gamma_{f_0 \rightarrow K^+K^- \rightarrow \gamma\gamma}^{\text{Born}}(m) \frac{3}{2} \\ &\times \left[\frac{m \Gamma_{f_0 \rightarrow \pi^+\pi^-}(m)}{\pi |D_{f_0}(m)|^2} \right] 2m dm \\ &= \frac{3}{2} \int_{m_1}^{m_2} \frac{m^2}{4\pi^2} \sigma_{f_0}(\gamma\gamma \rightarrow \pi^+\pi^-) dm \end{aligned} \quad (7)$$

[see also Eq. (2)]. This averaged width can serve as an adequate, working characteristic of the $f_0(980)$ coupling to $\gamma\gamma$. Substituting $\sigma_{f_0}(\gamma\gamma \rightarrow \pi^+\pi^-)$, shown in Figs. 2(b) and 2(c) in Eq. (7) and integrating, for example, over two m regions $0.93 \leq m \leq 1.03$ GeV and $2m_\pi \leq m < \infty$, we obtain $\langle \Gamma_{f_0 \rightarrow K^+K^- \rightarrow \gamma\gamma}^{\text{Born}} \rangle_{\pi\pi} \approx 0.114$ keV and 0.191 keV, respectively, for set A, 0.132 and 0.351 keV for set B, 0.129 and 0.211 keV for set C, and 0.152 and 0.377 keV for set D. Defining also $\langle \Gamma_{f_0 \rightarrow K^+K^- \rightarrow \gamma\gamma}^{\text{Born}} \rangle_{K\bar{K}}$ in a similar way, we find that the total averaged width of the $f_0 \rightarrow \gamma\gamma$ decay $\langle \Gamma_{f_0 \rightarrow K^+K^- \rightarrow \gamma\gamma}^{\text{Born}} \rangle = \langle \Gamma_{f_0 \rightarrow K^+K^- \rightarrow \gamma\gamma}^{\text{Born}} \rangle_{\pi\pi} + \langle \Gamma_{f_0 \rightarrow K^+K^- \rightarrow \gamma\gamma}^{\text{Born}} \rangle_{K\bar{K}} \approx 0.14$ keV and 0.359 keV for the two above mentioned integration regions, respectively, for set A, 0.164 and 0.884 keV for set B, 0.158 and 0.439 keV for set C, and 0.189 and 1.094 keV for set D. It is worth pointing out for comparison that $\Gamma_{f_0 \rightarrow K^+K^- \rightarrow \gamma\gamma}^{\text{Born}}(m)$ at the maximum, i.e., $\Gamma_{f_0 \rightarrow K^+K^- \rightarrow \gamma\gamma}^{\text{Born}}(2m_{K^+})$, is approximately equal to 0.589, 1.766, 0.785, and 2.355 keV for $g_{f_0 K\bar{K}}^2/16\pi$ from sets A, B, C, and D, respectively.

Certainly, the real situation in the $\gamma\gamma \rightarrow \pi^+\pi^-$ channel is more complicated because the $f_0(980)$ resonance in this channel is by no means a solitary one. It is accompanied by

the considerable coherent background, and therefore the interference effects are of great significance. Their role will be analyzed in detail below in Sec. III.

We wish to conclude this section with a general remark concerning the $f_0(980)$ resonance propagator, see Eq. (5), which we utilize throughout here. As is shown in Ref. [29], this propagator rigorously satisfies the Källén-Lehmann representation, i.e., it possesses the analytic properties required in field theory. Thus, the resonance mass distributions calculated with the use of this propagator are automatically normalized to the corresponding branching ratios of the $f_0(980) \rightarrow a\bar{a}$ decays, the sum of which is exactly equal to unit, i.e.,

$$\begin{aligned} \int_{2m_a}^{\infty} \left[\frac{m \Gamma_{f_0 \rightarrow a\bar{a}}(m)}{\pi |D_{f_0}(m)|^2} \right] 2m dm &= B(f_0(980) \rightarrow a\bar{a}), \\ \sum_{a\bar{a}} B(f_0(980) \rightarrow a\bar{a}) &= 1. \end{aligned}$$

III. S WAVE IN THE REACTION $\gamma\gamma \rightarrow \pi^+\pi^-$ NEAR 1 GEV

Let us consider the simplest dynamical model for the S wave amplitude of the reaction $\gamma\gamma \rightarrow \pi^+\pi^-$ in the 1 GeV region. There are no arbitrary, free parameters in this model (that is the parameters which would be unknown from other reactions), and within its framework the character of the interference between the background and $f_0(980)$ resonance contributions, and thus a possible resulting $f_0(980)$ shape in the $\gamma\gamma \rightarrow \pi^+\pi^-$ channel, will be fully elucidated. The results obtained in this way will be useful, in particular, as to estimate the potentialities and “price” of the more complicated model constructions.

Using the conventional normalization, we write the S wave cross section of the reaction $\gamma\gamma \rightarrow \pi^+\pi^-$, together with the corresponding amplitude $A_S(m)$, in the form:

$$\sigma_S(\gamma\gamma \rightarrow \pi^+\pi^-) = \frac{\rho_\pi(m)}{32\pi m^2} |A_S(m)|^2, \quad (8)$$

$$\begin{aligned} A_S(m) &= M_{\gamma\gamma \rightarrow \pi^+\pi^-}^{\text{Born}}(m) + 8\alpha I_{\pi^+\pi^-}(m) T_{\pi^+\pi^- \rightarrow \pi^+\pi^-}(m) \\ &+ 8\alpha I_{K^+K^-}(m) T_{K^+K^- \rightarrow \pi^+\pi^-}(m). \end{aligned} \quad (9)$$

Here

$$\begin{aligned} M_{\gamma\gamma \rightarrow \pi^+\pi^-}^{\text{Born}}(m) &= \frac{16\pi\alpha m_\pi^2}{m^2 \rho_\pi(m)} \ln \frac{1 + \rho_\pi(m)}{1 - \rho_\pi(m)} \\ &= \frac{8\alpha}{\rho_\pi(m)} \text{Im} I_{\pi^+\pi^-}(m) \end{aligned} \quad (10)$$

is the S wave Born amplitude of the process $\gamma\gamma \rightarrow \pi^+\pi^-$, the function $I_{\pi^+\pi^-}(m)$ results from Eq. (4) by replacing m_{K^+} and $\rho_{K^+}(m)$ by m_π and $\rho_\pi(m)$, respectively, and $T_{\pi^+\pi^- \rightarrow \pi^+\pi^-}(m)$ and $T_{K^+K^- \rightarrow \pi^+\pi^-}(m)$ are the S wave amplitudes of hadronic reactions indicated in their subscripts. Hence it is obvious that the second and third terms on the

right-hand side of Eq. (9) correspond to the contributions from the $\gamma\gamma \rightarrow \pi^+\pi^-$ and $\gamma\gamma \rightarrow K^+K^-$ Born amplitudes modified by the final state interactions. Such a structure of the amplitude $A_S(m)$ can be easily obtained within the framework of the field-theoretical model in which the electromagnetic Born amplitudes are the only primary sources of the $\pi^+\pi^-$ and K^+K^- pairs, and the strong amplitudes, used for unitarization of the Born contributions, are constructed by summing up all the s channel bubble diagrams. In so doing, the strong amplitudes can involve, in principle, any number of resonances plus background contributions to describe the relevant data on the phase shifts and inelasticities. The resulting strong and electromagnetic amplitudes in such a model are unitary. This model has a very old history [30,31] and up to now was successfully used, together with its dispersive modifications, as the effective tool in analyzing dynamics of electromagnetic and strong interaction processes; see for example [11,32–37].

The amplitude $T_{\pi^+\pi^-\rightarrow\pi^+\pi^-}(m)$ is related to the phase shifts $\delta_0^I(m)$ and inelasticities $\eta_0^I(m)$ of the S wave $\pi\pi$ scattering amplitudes with definite isospin $I = 0, 2$ in the conventional way: $T_{\pi^+\pi^-\rightarrow\pi^+\pi^-}(m) = \frac{2}{3}T_0^0(m) + \frac{1}{3}T_0^2(m)$, where $T_0^I(m) = \{\eta_0^I(m) \exp[2i\delta_0^I(m)] - 1\} / [2i\rho_\pi(m)]$. As is well known, the only, strongly coupled S wave channels in the 1 GeV region are the $\pi\pi$ and $K\bar{K}$ channels with $I = 0$. Therefore we set $\eta_0^2(m) = 1$ for all m of interest and $\eta_0^0(m) = 1$ for $m < 2m_{K^+}$. Then, for $m < 2m_{K^+}$, the amplitude $A_S(m)$ can be rewritten as, see Eqs. (9) and (10),

$$A_S(m) = e^{i\delta_0^0(m)} \{ A_{S,0}(m) + A_{S,2}(m) \cos[\delta_0^2(m) - \delta_0^0(m)] + iA_{S,2}(m) \sin[\delta_0^2(m) - \delta_0^0(m)] \}, \quad (11)$$

where the amplitudes $A_{S,I}(m)$ with $I = 0$ and 2 have the form:

$$A_{S,0}(m) = \frac{2}{3} M_{\gamma\gamma\rightarrow\pi^+\pi^-}^{\text{Born}}(m) \cos\delta_0^0(m) + [8\alpha/\rho_\pi(m)] \text{Re}[I_{\pi^+\pi^-}(m)] \frac{2}{3} \sin\delta_0^0(m) + 8\alpha I_{K^+K^-}(m) T_{K^+K^-\rightarrow\pi^+\pi^-}(m) e^{-i\delta_0^0(m)}, \quad (12)$$

$$A_{S,2}(m) = \frac{1}{3} \{ M_{\gamma\gamma\rightarrow\pi^+\pi^-}^{\text{Born}}(m) \cos\delta_0^2(m) + [8\alpha/\rho_\pi(m)] \text{Re}[I_{\pi^+\pi^-}(m)] \sin\delta_0^2(m) \}. \quad (13)$$

Because for $m < 2m_{K^+}$ the imaginary part of the function $I_{K^+K^-}(m)$ vanishes, see Eq. (4), and the phase of the amplitude $T_{K^+K^-\rightarrow\pi^+\pi^-}(m)$ reduces to $\delta_0^0(m) + n\pi$ (where $n = 0$ or 1) in accordance with unitarity, it is easy to see that all the terms in the amplitudes $A_{S,0}(m)$ and $A_{S,2}(m)$ are real. Moreover, all of these terms have well definite signs. Begin with the amplitude $T_{K^+K^-\rightarrow\pi^+\pi^-}(m) = T_{\pi^+\pi^-\rightarrow K^+K^-}(m)$ in Eq. (12). Its sign, $(-1)^n$, is known

experimentally and it is positive [24,38–41]. In terms of the $f_0(980)$ coupling constants this means that if we parametrize the amplitude $T_{K^+K^-\rightarrow\pi^+\pi^-}(m)$ in the 1 GeV region as [22,24,25]

$$T_{K^+K^-\rightarrow\pi^+\pi^-}(m) = \frac{g_{f_0\pi^+\pi^-} g_{f_0K^+K^-}}{16\pi D_{f_0}(m)} e^{i\delta_B(m)}, \quad (14)$$

where $\delta_B(m)$ is a smooth and large phase (of about 90° for $m \approx 1$ GeV) of the elastic background in the $I = 0$ S wave $\pi\pi$ channel, then the production $g_{f_0\pi^+\pi^-} g_{f_0K^+K^-}$ is positive [24,38,40]. Recall that with such a parametrization the $\pi\pi$ scattering amplitude $T_0^0(m)$ has the form [22–25]:

$$T_0^0(m) = \frac{\eta_0^0(m) e^{2i\delta_0^0(m)} - 1}{2i\rho_\pi(m)} = \frac{1}{\rho_\pi(m)} \left[\frac{e^{2i\delta_B(m)} - 1}{2i} + e^{2i\delta_B(m)} \frac{m\Gamma_{f_0\pi\pi}(m)}{D_{f_0}(m)} \right], \quad (15)$$

and that the $f_0(980)$ resonance appears as a dip in $|T_0^0(m)|$ [42]. Equations (14) and (15) will be used in the following. Thus, the last term on the right-hand side of Eq. (12) is positive because, according to Eq. (4), $I_{K^+K^-}(m) > 0$ for $0 < m \leq 2m_{K^+}$. Now we take into account the following circumstances. For $0.85 \text{ GeV} < m < 2m_{K^+}$, the phase shift $\delta_0^0(m)$ increases with m from 90° to about 200° sharply flying up near the K^+K^- threshold; see, for example, Ref. [43]. In the same region of m , the phase shift $\delta_0^2(m)$ is of about $-(19-24)^\circ$; see, for example, Ref. [44]. Moreover, $\text{Re}[I_{\pi^+\pi^-}(m)] < 0$ for $m > 0.376$ GeV. So, for $0.85 \text{ GeV} < m < 2m_{K^+}$, the first term on the right-hand side of Eq. (12) is negative, the second term is also negative at least up to 0.98 GeV, and it is small in magnitude for $0.98 \text{ GeV} < m < 2m_{K^+}$. Finally, it is easy to check that the amplitude $A_{S,2}(m) \cos[\delta_0^2(m) - \delta_0^0(m)]$, see Eqs. (11) and (13), is also negative for $0.85 \text{ GeV} < m < 2m_{K^+}$.

Thus, one can conclude that, for $m < 2m_{K^+}$, the sharply increasing with m , $f_0(980)$ production amplitude due to the K^+K^- loop mechanism has to interfere destructively with the accompanying background contributions in $\sigma_S(\gamma\gamma \rightarrow \pi^+\pi^-)$. Such an interference is able to suppress the left wing of the $f_0(980)$ resonance practically in full. A detailed illustration of the described general picture is presented in Fig. 3. In constructing the curves shown in this figure, we used set A for the values of the $f_0(980)$ resonance parameters and approximated the smooth phase shifts $\delta_B(m)$ and $\delta_0^2(m)$ by the following expressions: $\delta_B(m) = \rho_\pi(m) \sum_{n=0}^3 q_\pi^{2n}(m) a_{2n} = \rho_\pi(m) \times [0.1243 + q_\pi^2(m)16.32 - q_\pi^4(m)73.50 + q_\pi^6(m)118.3]$ and $\delta_0^2(m) = q_\pi(m) b_0 / [1 + \sum_{n=1}^3 q_\pi^{2n}(m) b_{2n}] = q_\pi(m) 0.9098 / [1 + q_\pi^2(m)2.629 - q_\pi^4(m)13.19 + q_\pi^6(m)18.83]$, where $\delta_B(m)$ and $\delta_0^2(m)$ in radians and $q_\pi(m) = m\rho_\pi(m)/2$ in

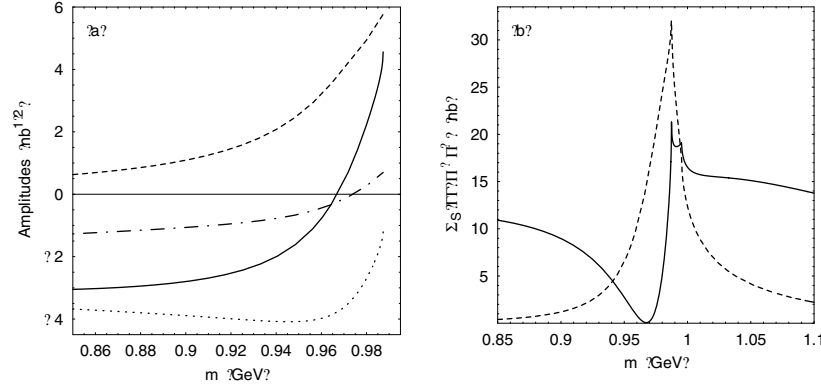


FIG. 3. (a) The components of the amplitude $\sqrt{\rho_\pi(m)/(32\pi m^2)}e^{-i\delta_0^0(m)}A_S(m)$ for $m \leq 2m_{K^+}$ are shown; see Eqs. (8), (9), and (11)–(13). The solid curve corresponds to the real part of this amplitude, which is added up of the $f_0(980)$ production amplitude due to the K^+K^- loop mechanism, shown by the dashed curve, and the real part of the sum of the background amplitudes, shown by the dotted curve. The dot-dashed curve corresponds to the imaginary part of this amplitude, which is stipulated only by the $I = 2$ contribution. (b) The solid curve shows the cross section $\sigma_S(\gamma\gamma \rightarrow \pi^+\pi^-)$ calculated by using Eqs. (8) and (9). The dashed curve shows the contribution to this cross section caused by the $f_0(980)$ production only via the K^+K^- loop mechanism. A comparison of these curves gives, in particular, a good idea of the important role of the interference between the background and resonance contributions. The values of the parameters utilized in constructing the curves in (a) and (b) correspond to set A, see the text.

units of GeV. Note that in this way we obtain the excellent description of the S wave $\pi\pi$ scattering data [43–45] at least in the m region from $2m_\pi$ up to 1.2 GeV (for example, according to our fit, the S wave $\pi\pi$ scattering length $a_0^0 \approx 0.229/m_\pi$). In Fig. 3(a) the solid curve shows that the real part of the amplitude $\sqrt{\rho_\pi(m)/(32\pi m^2)}e^{-i\delta_0^0(m)}A_S(m)$, see Eqs. (8), (9), and (11)–(13), vanishes at $m \approx 0.967$ GeV as a result of the compensation of the resonance and background contributions. As is seen from Fig. 3(b), this leads to a minimum in the cross section at the place of the left wing of the $f_0(980)$ resonance. As a whole, the resulting cross section $\sigma_S(\gamma\gamma \rightarrow \pi^+\pi^-)$ near 1 GeV in Fig. 3(b) resembles a step. Furthermore, we verified that sets B, C, and D for the $f_0(980)$ resonance parameters yield very similar results for $A_S(m)$ and $\sigma_S(\gamma\gamma \rightarrow \pi^+\pi^-)$.

To compare the model with the data pertaining to the partial solid angle, one must yet take into account the interference of the amplitude $A_S(m)$ with the higher partial waves. Usually, the measurements of the reaction $\gamma\gamma \rightarrow \pi^+\pi^-$ are performed in the angular region $|\cos\theta^*| < Z_0 < 1$. The $\gamma\gamma \rightarrow \pi^+\pi^-$ cross section is presented as the sum of the cross sections $\sigma_{\lambda=0}(\gamma\gamma \rightarrow \pi^+\pi^-, |\cos\theta^*| < Z_0)$ and $\sigma_{|\lambda|=2}(\gamma\gamma \rightarrow \pi^+\pi^-, |\cos\theta^*| < Z_0)$, where λ is a photon helicity difference. In the $Z_0 < 1$ case, all the partial waves interfere between themselves in both cross sections. The cross section with $|\lambda| = 2$ is dominated by the D wave Born contribution and the well-known $f_2(1270)$ resonance [1–3,34]. The $f_2(1270)$ coupling to the $\gamma\gamma$ system in the $\lambda = 0$ state is small [2,34]. Therefore, we assume for estimate that in the 1 GeV region all the higher partial waves with $\lambda = 0$ are defined simply by the corresponding $\gamma\gamma \rightarrow \pi^+\pi^-$ Born amplitude. Then, $\sigma_{\lambda=0}(\gamma\gamma \rightarrow \pi^+\pi^-, |\cos\theta^*| < Z_0)$ can be written in the form:

$$\begin{aligned} \sigma_{\lambda=0}(\gamma\gamma \rightarrow \pi^+\pi^-, |\cos\theta^*| < Z_0) &= \frac{\rho_\pi(m)}{32\pi m^2} \left\{ Z_0 |\tilde{A}_S(m)|^2 + C \operatorname{Re}[\tilde{A}_S(m)] \frac{1}{\rho_\pi(m)} \right. \\ &\quad \times \ln \frac{1 + Z_0 \rho_\pi(m)}{1 - Z_0 \rho_\pi(m)} + C^2 \left[\frac{Z_0/2}{1 - Z_0^2 \rho_\pi^2(m)} \right. \\ &\quad \left. \left. + \frac{1}{4\rho_\pi(m)} \ln \frac{1 + Z_0 \rho_\pi(m)}{1 - Z_0 \rho_\pi(m)} \right] \right\}, \end{aligned} \quad (16)$$

where the amplitude $\tilde{A}_S(m) = A_S(m) - M_{\gamma\gamma \rightarrow \pi^+\pi^-}^{\text{Born}}(m)$, see Eq. (9), and $C = 32\pi\alpha m_\pi^2/m^2$. With the use of Eq. (16), one can easily verify that for the typical value of $Z_0 = 0.6$ the higher partial wave influence, certainly, exists, but it is not too large.

Figures 4(a) and 4(b) illustrate the comparison of the model predictions for $\sigma(\gamma\gamma \rightarrow \pi^+\pi^-, |\cos\theta^*| < 0.6) = \sigma_{\lambda=0}(\gamma\gamma \rightarrow \pi^+\pi^-, |\cos\theta^*| < 0.6) + \sigma_{|\lambda|=2}(\gamma\gamma \rightarrow \pi^+\pi^-, |\cos\theta^*| < 0.6)$ with the Belle data in the $f_0(980)$ resonance region. To obtain the curves in Fig. 4(a), we performed the simultaneous fit to the Belle data [1] and the well-known S wave $\pi\pi$ scattering data from Refs. [43,45]. In so doing, we used Eqs. (9), (10), and (14)–(16), the above mentioned expression for $T_0^2(m)$, and the approximation of the cross section with $|\lambda| = 2$ by a linear function of m , $C_1 + C_2 m$ [of course, this is a reasonable approximation only in the considered, narrow region of m around the $f_0(980)$ resonance]. The parameters obtained (set E) are $m_{f_0} = 0.9676$ GeV, $g_{f_0\pi\pi}^2/16\pi = 0.07017$ GeV², $g_{f_0K\bar{K}}^2/16\pi = 0.3442$ GeV² ($R = 4.9$), $C_1 = 57.69$ nb, $C_2 = 23.45$ nb/GeV, and $a_{2n=0,2,4,6} = 0.1404, 17.17, -80.17, 127.4$, respectively. In order to illustrate that the Belle data tolerate, in fact, the wide range

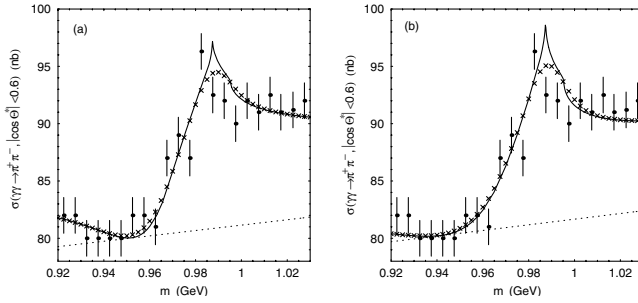


FIG. 4. The comparison of the model predictions for the cross section $\sigma(\gamma\gamma \rightarrow \pi^+\pi^-, |\cos\theta^*| < 0.6) = \sigma_{\lambda=0}(\gamma\gamma \rightarrow \pi^+\pi^-, |\cos\theta^*| < 0.6) + \sigma_{|\lambda|=2}(\gamma\gamma \rightarrow \pi^+\pi^-, |\cos\theta^*| < 0.6)$ with the Belle data [from Fig. 1(b)] in the $f_0(980)$ resonance region. (a) The solid curve, crosses, and dotted line show the cross section without and with a Gaussian mass smearing (with the dispersion of 5 MeV), and the contribution of the $|\lambda| = 2$ cross section approximated by a linear function of m , respectively. The presented fit [obtained, in particular, with use of Eqs. (9), (10), and (14)–(16)] corresponds to the model parameters from set E, see the text. (b) The same as in (a) but for the model parameters from set F.

for the $f_0(980)$ coupling constant values, we fixed $g_{f_0 K\bar{K}}^2/16\pi = 1.6 \text{ GeV}^2$ and performed once again the fit to the above mentioned data. For this case, the parameters obtained (set F) are $m_{f_0} = 0.968 \text{ GeV}$, $g_{f_0 \pi\pi}^2/16\pi = 0.2438 \text{ GeV}^2$ ($R = 6.56$), $C_1 = 57.05 \text{ nb}$, $C_2 = 24.62 \text{ nb/GeV}$, and $a_{2n=0,2,4,6} = 0.01903, 18.13, -96.71, 173.2$, respectively, and the resulting picture is shown in Fig. 4(b). As a whole, we obtain the quite satisfactory, qualitative agreement with the data in both the magnitude and shape of the $f_0(980)$ resonance manifestation. The strong difference of the $f_0(980)$ resonance shape in the $\gamma\gamma \rightarrow \pi^+\pi^-$ reaction cross section from the shape of the solitary Breit-Wigner resonance is a result of fine interference effects between the different contributions. As we have made sure, the considered dynamical model provides a fairly good basis for understanding these effects. The model unambiguously points to the destructive interference pattern between the resonance and background contributions in the m region below the K^+K^- threshold.

Now we discuss, in brief, a possible manifestation of the $f_0(980)$ resonance in the S wave $\gamma\gamma \rightarrow \pi^0\pi^0$ reaction cross section. In the considered model we have

$$\sigma_S(\gamma\gamma \rightarrow \pi^0\pi^0) = \frac{\rho_\pi(m)}{64\pi m^2} |B_S(m)|^2, \quad (17)$$

$$B_S(m) = 8\alpha I_{\pi^+\pi^-}(m) T_{\pi^+\pi^- \rightarrow \pi^0\pi^0}(m) + 8\alpha I_{K^+K^-}(m) T_{K^+K^- \rightarrow \pi^0\pi^0}(m), \quad (18)$$

where $T_{\pi^+\pi^- \rightarrow \pi^0\pi^0}(m) = \frac{2}{3}T_0^0(m) - \frac{2}{3}T_0^2(m)$ and $T_{K^+K^- \rightarrow \pi^0\pi^0}(m) = T_{K^+K^- \rightarrow \pi^+\pi^-}(m)$. In comparison with

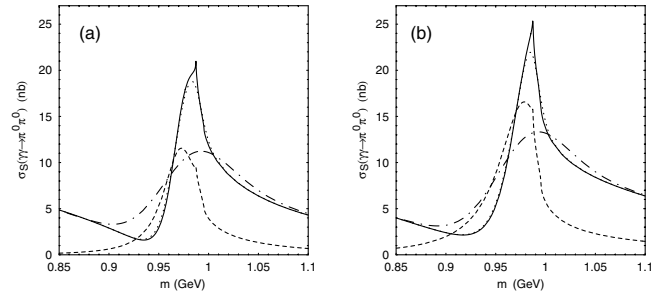


FIG. 5. (a) The solid curve shows the cross section $\sigma_S(\gamma\gamma \rightarrow \pi^0\pi^0)$ calculated with use of Eqs. (17) and (18) in the case of the model parameters from set E. The dotted and dot-dashed curves show the same cross section but smoothed with a Gaussian mass distribution with the dispersion of 5 and 30 MeV, respectively. The dashed curve shows the contribution caused by the $f_0(980)$ resonance production via the K^+K^- loop mechanism only. (b) The same as in (a) but for the model parameters from set F.

the amplitude $A_S(m)$, see Eq. (9), the amplitude $B_S(m)$ does not contain the Born term and the $T_0^2(m)$ amplitude contribution is doubled and has the opposite sign. These differences are essential. As is seen from Fig. 5, the $f_0(980)$ resonance in the $\gamma\gamma \rightarrow \pi^0\pi^0$ channel has to manifest itself as a distinct peak. In this respect, the reaction $\gamma\gamma \rightarrow \pi^0\pi^0$, generally speaking, is more preferred than the reaction $\gamma\gamma \rightarrow \pi^+\pi^-$. Unfortunately, in the Crystal Ball [5,6] and JADE [7] experiments, the $\gamma\gamma \rightarrow \pi^0\pi^0$ cross section was scanned with a 50-MeV and 30-MeV-wide step, respectively. Such a mass resolution is still lacking to discover the $f_0(980)$ peak. Figures 5(a) and 5(b) show, in particular, that a Gaussian smearing with the dispersion of 30 MeV leaves nothing from the specific features of the $f_0(980)$ peak in $\sigma_S(\gamma\gamma \rightarrow \pi^0\pi^0)$. Notice, that there are no contradictions between the presented estimate for the smoothed $\sigma_S(\gamma\gamma \rightarrow \pi^0\pi^0)$ and the normalized Crystal Ball data [5,6] for $\sigma(\gamma\gamma \rightarrow \pi^0\pi^0, |\cos\theta^*| < 0.8, 0.7)$.

Of course, the considered model allows us to predict the S wave $\gamma\gamma \rightarrow \pi\pi$ reaction cross sections for a more wide region of m than the neighborhood of the $f_0(980)$ resonance. The corresponding cross sections $\sigma_S(\gamma\gamma \rightarrow \pi^+\pi^-)$ and $\sigma_S(\gamma\gamma \rightarrow \pi^0\pi^0, |\cos\theta^*| < 0.8)$ in the m region from $2m_\pi$ to 1.2 GeV are shown in Fig. 6 for the model parameters corresponding to sets E and F. Unfortunately, in such a wide m interval we cannot directly compare the predictions for $\sigma_S(\gamma\gamma \rightarrow \pi\pi)$ with experiment, because this requires the accurate S wave data obtained by separating highest partial waves with the use of a partial wave analysis of the reaction events. For example, in the reaction $\gamma\gamma \rightarrow \pi^+\pi^-$, the D wave contribution with $|\lambda| = 2$ can constitute from 75% to 90% of the total cross section for $m > 0.5 \text{ GeV}$. In the $\gamma\gamma \rightarrow \pi^0\pi^0$ channel, the D wave contribution, caused in the main by the $f_2(1270)$ resonance, is also very important for $m > 0.85 \text{ GeV}$, as is clear from Fig. 6(c).

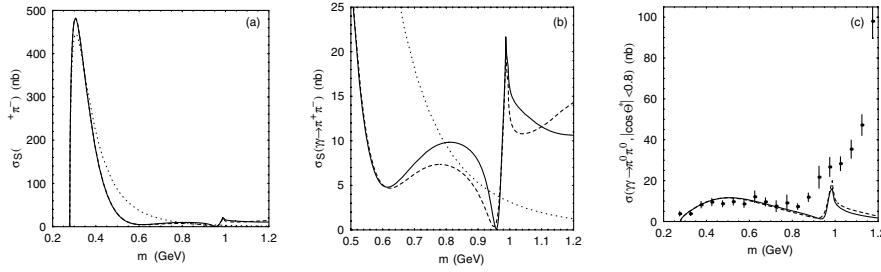


FIG. 6. The S wave cross sections $\sigma_S(\gamma\gamma \rightarrow \pi^+\pi^-)$, in (a) and (b), and $\sigma_S(\gamma\gamma \rightarrow \pi^0\pi^0, |\cos\theta^*| < 0.8)$, in (c), obtained in the considered model for the wide regions of m . They are shown by the solid and dashed curves corresponding to the model parameters from sets E and F, respectively. The dotted curves in (a) and (b) correspond to the S wave Born contribution. The experimental points in (c) are the Crystal Ball data on $\sigma(\gamma\gamma \rightarrow \pi^0\pi^0, |\cos\theta^*| < 0.8)$ [5] (the quoted errors are statistical only); the rise of the measured cross section for $m > 0.8$ GeV is due to the $f_2(1270)$ resonance contribution [5].

Hence, the thorough separation of the large D wave background is of crucial importance for the extraction of the S wave in both reactions.

Finally, we wish to say a few words about ambiguities which, in fact, inevitably occur in theoretical models for the amplitudes of electromagnetic interactions of hadrons. Concretely, we bear in mind rather evident possibilities of the incorporation of some unknown, free parameters into the aforesaid model. One of these parameters is the so-called direct $f_0(980) \rightarrow \gamma\gamma$ coupling constant, $g_{f_0 \rightarrow \gamma\gamma}^0$. Taking account of this constant, the corresponding total amplitude of the $f_0 \rightarrow \gamma\gamma$ decay can be written as $M_{f_0 \rightarrow \gamma\gamma}(m) = M_{f_0 \rightarrow K^+K^- \rightarrow \gamma\gamma}^{\text{Born}}(m) + g_{f_0 \rightarrow \gamma\gamma}^0$, where $M_{f_0 \rightarrow K^+K^- \rightarrow \gamma\gamma}^{\text{Born}}(m)$ is the amplitude due to the Born K^+K^- loop mechanism from Eq. (3). Of course, for any mechanism, the two-photon decay amplitude of any scalar meson must be proportional to m^2 for $m \rightarrow 0$, as, for example, the Born amplitude $M_{f_0 \rightarrow K^+K^- \rightarrow \gamma\gamma}^{\text{Born}}(m)$. However, if we are interested in only the narrow m region around 1 GeV, the adding of the constant $g_{f_0 \rightarrow \gamma\gamma}^0$ to $M_{f_0 \rightarrow K^+K^- \rightarrow \gamma\gamma}^{\text{Born}}(m)$ is a quite reasonable approximation. About the coupling constant $g_{f_0 \rightarrow \gamma\gamma}^0$ one can say as follows. It can have neither the value comparable in magnitude and coincident in sign with the value of $M_{f_0 \rightarrow K^+K^- \rightarrow \gamma\gamma}^{\text{Born}}(m)$ at the maximum, i.e., with $M_{f_0 \rightarrow K^+K^- \rightarrow \gamma\gamma}^{\text{Born}}(2m_{K^+}) = \alpha(\pi^2/4 - 1)g_{f_0 K^+K^-}/2\pi$, nor the value comparable in magnitude but opposite in sign with $M_{f_0 \rightarrow K^+K^- \rightarrow \gamma\gamma}^{\text{Born}}(2m_{K^+})$, since otherwise the $\gamma\gamma \rightarrow \pi^+\pi^-$ reaction cross section in the $f_0(980)$ region would be in sharp contradiction with the data, in both magnitude and shape. Moreover, there is no evidence for the presence of the pointlike $f_0(980)\phi\gamma$ interaction from the data on the $\phi \rightarrow \pi\pi\gamma$ decays [12–14,20]. Actually, the experiment tells us that the direct $f_0 \rightarrow \gamma\gamma$ coupling seems to be small. Any reliable theoretical estimates for this coupling have not existed yet. Serious experimental and theoretical searches for its signs together with those of the direct

coupling of the $f_0(600)/\sigma$ to $\gamma\gamma$ are still a matter of the future.

IV. CONCLUSION

The present analysis was stimulated by the Belle data [1]. The main results consist in the following.

(i) It has been shown that the K^+K^- loop mechanism provides the absolutely natural and reasonable scale of the $f_0(980)$ resonance manifestation in the $\gamma\gamma \rightarrow \pi^+\pi^-$ and $\gamma\gamma \rightarrow \pi^0\pi^0$ reaction cross sections.

(ii) It has been shown that the shape of the $f_0(980)$ resonance in the reaction $\gamma\gamma \rightarrow \pi^+\pi^-$ has nothing to do with the shape of a solitary Breit-Wigner resonance. This result is supported by the Belle data. In so doing, the observed pattern of the $f_0(980)$ peak distortion can be easily explained with use of the simple dynamical model.

Certainly, for a more full understanding of the situation, the information based on a partial wave analysis of the $\gamma\gamma \rightarrow \pi^+\pi^-$ reaction events in the $f_0(980)$ resonance region would be extremely useful. The huge statistics collected in the Belle experiment [1], in principle, allows one to hope for the successful performance of such an analysis.

It is clear from the preceding discussion that high quality data on the reaction $\gamma\gamma \rightarrow \pi^0\pi^0$ would be also highly desirable, because the relative role of the background contributions in the $f_0(980)$ region in this channel is considerably smaller than in the charged one.

The new stage of high statistics measurements of the processes $\gamma\gamma \rightarrow \pi^+\pi^-$, $\gamma\gamma \rightarrow \pi^0\pi^0$, $\gamma\gamma \rightarrow \eta\pi^0$, $\gamma\gamma \rightarrow K^+K^-$, and $\gamma\gamma \rightarrow K^0\bar{K}^0$, begun by the Belle Collaboration, undoubtedly, will serve the further progress of physics of light scalar mesons.

ACKNOWLEDGMENTS

This work was supported in part by the Presidential Grant No. 2339.2003.2 for the support of Leading Scientific Schools.

- [1] T. Mori *et al.* (Belle Collaboration), in *Proceedings of the International Symposium on Hadron Spectroscopy Chiral Symmetry and Relativistic Description of Bound Systems, Tokyo, 2003*, edited by S. Ishida, K. Takamatsu, T. Tsuru, S. Y. Tsai, M. Ishida, and T. Komada (KEK Proceedings 2003-7, 2003) (KEK, Tsukuba, 2003), p. 159.
- [2] J. Boyer *et al.*, Phys. Rev. D **42**, 1350 (1990).
- [3] H. J. Behrend *et al.*, Z. Phys. C **56**, 381 (1992).
- [4] R. Barate *et al.*, Phys. Lett. B **472**, 189 (2000).
- [5] H. Marsiske *et al.*, Phys. Rev. D **41**, 3324 (1990).
- [6] J. K. Bienlein, in *Proceedings of the IX International Workshop on Photon-Photon Collisions, San Diego, 1992*, edited by D. Caldwell and H. P. Paar (World Scientific, Singapore, 1992), p. 241; D. Morgan, M. R. Pennington, and M. R. Whalley, J. Phys. G **20**, A1 (1994).
- [7] T. Oest *et al.*, Z. Phys. C **47**, 343 (1990).
- [8] M. Boglione and M. R. Pennington, Eur. Phys. J. C **9**, 11 (1999).
- [9] N. N. Achasov and V. N. Ivanchenko, Nucl. Phys. **B315**, 465 (1989).
- [10] N. N. Achasov and V. V. Gubin, Phys. Rev. D **56**, 4084 (1997); **63**, 094007 (2001); Yad. Fiz. **65**, 1566 (2002) [Phys. At. Nucl. **65**, 1528 (2002)].
- [11] N. N. Achasov and V. V. Gubin, Phys. Rev. D **57**, 1987 (1998); Yad. Fiz. **61**, 1473 (1998) [Phys. At. Nucl. **61**, 1367 (1998)].
- [12] M. N. Achasov *et al.*, Phys. Lett. B **440**, 442 (1998); **485**, 349 (2000).
- [13] R. R. Akhmetshin *et al.*, Phys. Lett. B **462**, 380 (1999).
- [14] A. Aloisio *et al.*, Phys. Lett. B **537**, 21 (2002).
- [15] M. N. Achasov *et al.*, Phys. Lett. B **438**, 441 (1998); **479**, 53 (2000).
- [16] A. Aloisio *et al.*, Phys. Lett. B **536**, 209 (2002).
- [17] N. N. Achasov and A. V. Kiselev, Phys. Rev. D **68**, 014006 (2003); Yad. Fiz. **67**, 653 (2004) [Phys. At. Nucl. **67**, 633 (2004)].
- [18] N. N. Achasov and G. N. Shestakov, Z. Phys. C **41**, 309 (1988).
- [19] N. N. Achasov, Usp. Fiz. Nauk **168**, 1257 (1998) [Phys. Usp. **41**, 1149 (1998)]; Nucl. Phys. **A675**, 279c (2000); Yad. Fiz. **65**, 573 (2002) [Phys. At. Nucl. **65**, 546 (2002)].
- [20] N. N. Achasov, Nucl. Phys. **A728**, 425 (2003); Yad. Fiz. **67**, 1552 (2004) [Phys. At. Nucl. **67**, 1529 (2004)].
- [21] N. N. Achasov, S. A. Devyanin, and G. N. Shestakov, Phys. Lett. **108B**, 134 (1982); Z. Phys. C **16**, 55 (1982).
- [22] N. N. Achasov, S. A. Devyanin, and G. N. Shestakov, Yad. Fiz. **32**, 1098 (1980) [Sov. J. Nucl. Phys. **32**, 566 (1980)]; Z. Phys. C **22**, 53 (1984); Usp. Fiz. Nauk **142**, 361 (1984) [Sov. Phys. Usp. **27**, 161 (1984)].
- [23] S. M. Flatte, Phys. Lett. **63B**, 228 (1976).
- [24] A. D. Martin, E. N. Ozmutlu, and E. J. Squires, Nucl. Phys. **B121**, 514 (1977).
- [25] N. N. Achasov and G. N. Shestakov, Phys. Rev. D **58**, 054011 (1998); Yad. Fiz. **62**, 548 (1999) [Phys. At. Nucl. **62**, 505 (1999)].
- [26] P. Colangelo and F. De Fazio, Phys. Lett. B **559**, 49 (2003).
- [27] M. Ablikim *et al.*, Phys. Lett. B **607**, 243 (2005).
- [28] S. Eidelman *et al.* (Particle Data Group), Phys. Lett. B **592**, 1 (2004).
- [29] N. N. Achasov and A. V. Kiselev, Phys. Rev. D **70**, 111901 (2004).
- [30] F. Zachariassen, Phys. Rev. **121**, 1851 (1961); *High-Energy Physics and Elementary Particles* (IAEA, Vienna, 1965), p. 823; M. Gell-Mann and F. Zachariassen, Phys. Rev. **124**, 953 (1961).
- [31] W. Thirring, Phys. Rev. **126**, 1209 (1962); *Theoretical Physics* (IAEA, Vienna, 1963), p. 451.
- [32] L. S. Brown and R. L. Goble, Phys. Rev. Lett. **20**, 346 (1968); R. L. Goble and J. L. Rosner, Phys. Rev. D **5**, 2345 (1972).
- [33] G. Mennessier, Z. Phys. C **16**, 241 (1983).
- [34] R. P. Johnson, Ph.D. thesis, SLAC (SLAC Report No. 294, 1986).
- [35] R. L. Goble, R. Rosenfeld, and J. L. Rosner, Phys. Rev. D **39**, 3264 (1989); D. Morgan and M. R. Pennington, Phys. Lett. B **272**, 134 (1991); J. F. Donoghue and B. R. Holstein, Phys. Rev. D **48**, 137 (1993).
- [36] N. N. Achasov and G. N. Shestakov, Phys. Rev. D **49**, 5779 (1994); Yad. Fiz. **56**, 206 (1993) [Phys. At. Nucl. **56**, 1270 (1993)]; Int. J. Mod. Phys. A **9**, 3669 (1994).
- [37] N. N. Achasov and G. N. Shestakov, Phys. Rev. D **63**, 014017 (2001); Yad. Fiz. **65**, 579 (2002) [Phys. At. Nucl. **65**, 552 (2002)].
- [38] D. Morgan, Phys. Lett. **51B**, 71 (1974).
- [39] W. Wetzel *et al.*, Nucl. Phys. **B115**, 208 (1976).
- [40] P. Estabrooks, Phys. Rev. D **19**, 2678 (1979).
- [41] D. Cohen *et al.*, Phys. Rev. D **22**, 2595 (1980).
- [42] Here it should be noted that the $\pi^+\pi^-$ intermediate state contribution to the $f_0(980) \rightarrow \gamma\gamma$ decay width makes no sense by itself in contrast to the K^+K^- one. This is so because the contributions to the $\gamma\gamma \rightarrow \pi^+\pi^-$ amplitude $A_S(m)$ from the $f_0(980)$ resonance production via the $\pi^+\pi^-$ intermediate state and the smooth, large elastic $\pi^+\pi^-$ background cancel each other completely at $m \approx m_{f_0}$ in the second term in Eq. (9), see also Eqs. (11), (12), and (15) and $[\delta_0^0(m) \approx 180^\circ$ at this point]. Nevertheless, as described below, the wings of this term outside of its minimal value, together with the Born term in Eq. (9), strongly interfere in the cross section with the third resonance term from Eq. (9).
- [43] B. Hyams *et al.*, Nucl. Phys. **B64**, 134 (1973); G. Grayer *et al.*, Nucl. Phys. **B75**, 189 (1974); P. Estabrooks and A. D. Martin, Nucl. Phys. **B79**, 301 (1974).
- [44] W. Hoogland *et al.*, Nucl. Phys. **B126**, 109 (1977); N. B. Durusoy *et al.*, Phys. Lett. **45B**, 517 (1973).
- [45] L. Rosselet *et al.*, Phys. Rev. D **15**, 574 (1977); A. A. Bel'kov *et al.*, Pis'ma Zh. Eksp. Teor. Fiz. **29**, 652 (1979) [JETP Lett. **29**, 597 (1979)]; K. N. Mukhin *et al.*, Pis'ma Zh. Eksp. Teor. Fiz. **32**, 616 (1980) [JETP Lett. **32**, 601 (1980)]; S. Pislak *et al.*, Phys. Rev. Lett. **87**, 221801 (2001).